REPORT DOCUMENTATION PAGE

Form Approved
OMB No. 0704-0188

1. REPORT DATE *(DD-MM-YYYY)*	**2. REPORT TYPE** Technical Paper	**3. DATES COVERED** *(From - To)* See Attached List
4. TITLE AND SUBTITLE See Attached List		**5a. CONTRACT NUMBER** N/A **5b. GRANT NUMBER** N/A **5c. PROGRAM ELEMENT NUMBER** N/A
6. AUTHOR(S) See Attached List		**5d. PROJECT NUMBER** N/A **5e. TASK NUMBER** N/A **5f. WORK UNIT NUMBER** N/A
7. PERFORMING ORGANIZATION NAME(S) AND ADDRESS(ES) See Attached List		**8. PERFORMING ORGANIZATION REPORT NUMBER** N/A
9. SPONSORING / MONITORING AGENCY NAME(S) AND ADDRESS(ES) Kristi Laug AFRL/PROP 1950 Fifth Street Wright-Patterson AFB OH 45433 937-255-3362		**10. SPONSOR/MONITOR'S ACRONYM(S)** N/A **11. SPONSOR/MONITOR'S REPORT NUMBER(S)** N/A

12. DISTRIBUTION / AVAILABILITY STATEMENT

Distribution Statement A: Approved for public release; distribution is unlimited.

13. SUPPLEMENTARY NOTES

N/A

14. ABSTRACT

20030113 089

15. SUBJECT TERMS

16. SECURITY CLASSIFICATION OF: UNCLASSIFIED			**17. LIMITATION OF ABSTRACT**	**18. NUMBER OF PAGES**	**19a. NAME OF RESPONSIBLE PERSON** Kristi Laug
a. REPORT	**b. ABSTRACT**	**c. THIS PAGE**	Unlimited Distribution	See Attached List	**19b. TELEPHONE NUMBER** *(include area code)* 937-255-3362

TITLE	AUTHORS	DATES	PAGES
The Place of Solar Thermal Rockets in space	C. C. Selph	May 81	24
Solar Thermal Propulsion from Concept to Reality	Karl J. Iliev	Aug 1996	11
Solar BI-Modal System Concept: Mission Applications, A Preliminary Assessment	Kristi K. Laug, Michael R. Holmes Kurt O. Westerman		5
Dual-Propulsion Technology Reusable Orbit Transfer Vehicle Study	Travis Elkins, Terence Galati		7
Studies of Hafnium-Carbide Wafers using a Thermogravimetric	Domingo G. Castillo, Paul F. Jones		11
One Dimensional Model of a Solar-Thermal Thruster Using a Porous Absorber/Heat Exchanger	Michael R. Holmes	October 15, 1993	29
Evaluation of Hafnium-Carbide Wafers for use in a Solar Calorimeter	Kristi K. Laug, Alan J. Baxter		7
Solar Thermal Propulsion Experiments Design	Kristi K. Laug	1996	11
Porous Disk Test Bed Report of Results	Richard Hurtz	Aug 10, 1990	24
The Solar Propulsion Concept is Alive and Well at the Astronautics Laboratory	Kristi K. Laug	Nov 26, 1993	70
Foam Inflated Rigidized Truss Structure Developed for an SRS Technologies Solar Concentrator	Dean M. Lester, David M. Cannon	1996	8
Fabrication of Thin Film Concentrators for Solar Thermal Propulsion Applications	Paul A. Cierow	1991	7
Scaling Characteristics of Inflatable Paraboloid Concentrators	Mitchell Thomas, Gordon Veal	1991	6
AFRPL Solar-Thermal Rocket Activities	C.C. Selph, G.J. Naujokas	March 1984	9
Dependence of Solar-Thermal Rocket Performance on Çoncentrator Performance	Michael R. Holmes, Kristi K. Laug	1995	12
A Comparison of the Performance of Seamed and unseamed Inflatable Concentrators	Arthur Palisoc, Mitchell Thomas	1995	10
Society for the Advancement of Material and Process Engineering	Thomas C. Walton, James V. Crivello		10
Ideal Performance of Off-Axis Paraboloid Concentrators for Solar Thermal Propulsion	Michael R. Holmes		7
A Performance Evaluation of an Inflatable Concentrator for Solar Thermal Propulsion	J.P. Paxton, M. R. Holmes		10
Prediction of the Response of a Polyimide Concentrator for Solar Thermal Propulsion	Paul A. Gierow, William R. Clayton, James D. Moore		8
Inflatable Concentrators for Solar Themal Proulsion	William R. Clayton, Paul A. Gierow	1992	6
The Long Term Storability and Expulsion ofRocket Propellants and Oxidizers	Gordon David Elder	Aug 13, 1987	5
Prediction of the Response of a PolyimideConcentrator forSolar Thermal Propulsion	Paul A. Gierow, James D. Moore		11
Conceptual Design Study of a Solar Concentrator	R. Prasinghe, Kristi K. Laug		13
PL (OLAC)/RKAS Concentrator Information	Michael R. Holmes	Feb 11, 1993	29
Dependence of Solar-Thermal Rocket Performance on Concentrator Performance	Michael R. Holmes, Kristi K. Laug	1995	12
Thruster Interface	Michael R. Holmes	May 4, 1994	23
Cumulative Power Plots	Kristi K. Laug		87

SOLAR THERMAL PROPULSION EXPERIMENTS DESIGN

Kristi K. Laug
OL-AC PL/RKES
Edwards AFB CA 93524-7190
(805) 275-5127

ABSTRACT

Satellites that are currently under powered or have low photovoltaic (PV) efficiency, may be rejuvenated by dosing them with laser power beamed from earth. Also, current strictly solar thermal propulsion schemes may be able to use laser power as a replacement energy source when they are eclipsed. Several questions must be answered before a multiple use of laser power may be designated. The questions are outlined in the background section of this paper. They deal with gains that may be realized using solar power for operating specific hardware as opposed to laser power. A series of experiments that will give us information we can use to answer the questions will be performed. However, this paper outlines and presents only the design of experiments based upon statistical methods generated by Dr. Genuchi Taguchi.

INTRODUCTION

This paper is focused on the solar thermal experimental matrix and the design thereof that will be used to set up the experiments. Some simple laser power beaming experiments on existing solar thermal propulsion hardware were already performed.[1] Experiments using solar energy as the power source on the very same hardware will soon be performed. The data will be compared to determine differences in performance.

OBJECTIVE

The overall goal is to determine the feasibility of using OL-AC Phillips Laboratory (PL)/RKES's reticulated vitreous carbon calorimeter (RVCC) as a Solar and Laser Powered Rocket Engine (SLPRE). A Solar and Laser Powered Rocket Engine is a propulsion device which consists of a structure with a cavity or surface where either solar or laser energy is focused and captured as thermal energy. This energy is then transferred to a working fluid such as helium or hydrogen. Once the working fluid is heated by the thermal energy it is expanded through a nozzle, producing thrust (kinetic energy).

The testing goal is to collect data for our thruster modeling. Testing this engine will add important data to the modeled engines database at little cost to OL-AC PL/RKES. Experiments will be performed on the RVCC in the solar furnace at Phillips Lab, Edwards AFB; data collected will be compared with data accumulated during testing in the Chemical Oxygen Iodine Laser (COIL) at Kirtland AFB NM.[2]

Another goal is to fabricate and fly the solar/laser rocket engine in space. Eventually, one of the SLPREs will undergo exhaustive reliability and maintainability testing at flight conditions in preparation for a space flight test mission from Low Earth Orbit to Geosynchronous Earth Orbit. See the figures below. Fig. 1 is our rendering of a solar powered rocket in space. Fig. 2 is a schematic of the solar powered rocket in Fig. 1.

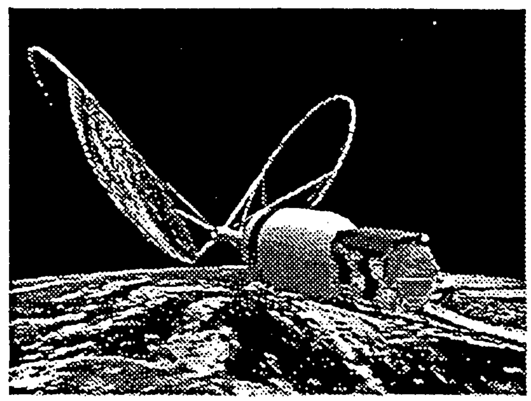

Fig. 1 Solar Powered Rocket

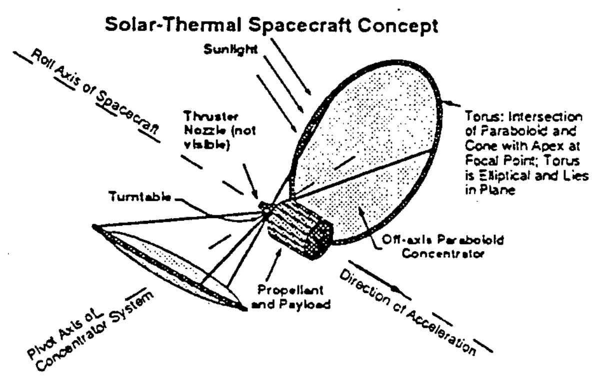

Fig. 2 Solar Thermal Rocket Propulsion Mission Scenario

[1] Kristi K. Laug and John David Holtzclaw, Volumetric Absorber as Solar Engine Utilizing Laser Thermal Power for Energy Input. 1995 Joint Army Navy NASA Air Force (JANNAF) Propulsion Meeting Proceedings, CPIA Publication, Tampa FL, 4-8 December 1995.

[2] Laug & Holtzclaw, Volumetric Absorber as Solar Engine Utilizing Laser Thermal Power for Energy Input.

The questions which must be answered in order to achieve the goals are: Can current propulsion schemes benefit from using laser and solar power beaming? Can a solar thermal propulsion system use laser power beaming for its primary energy source and visa versa? Sunlight exists in seemingly inexhaustible quantities. Even after laser power beaming is weakened and diffused to the point of inexistence over many thousands of kilometers, sunlight will still be able to be concentrated and focused enough to produce enough heat to propel a solar rocket. It lends itself well for interplanetary missions. Chemical rockets will be slower than solar for interplanetary missions because they thrust once and coast. Solar rockets will still thrust repeatedly, resulting in faster, cheaper trip times for the customer. Can current facilities and personnel be used to experimentally validate the concept? This is the main area Taguchi's Design of Experiments methods can help.[3] The method determines the important variables needed to be considered, how all the variables interact with each other, and how to perform the fewest number of experiments while gaining the most knowledge.

BACKGROUND

The Phillips Lab Propulsion Directorate: Participates in the research and development of a wide range of solar, laser, and bi-modal hybrid propulsion systems for upper stage orbital transfer vehicles. Wants to improve system capability by introducing advanced solar upper stage or orbital transfer vehicle propulsion concepts. Has conceptualized, designed and analyzed innovative approaches for SLPREs. Is in the process of developing and fabricating one or more SLPRE prototypes.

OL-AC PL/RKES: Maintains the Air Force Solar Laboratory Facility at Edwards AFB in California, it is a state-of-the-art, solar-powered test facility complete with a vacuum system which is capable of simulating altitude required to conduct controlled tests of solar energy usable hardware. Employs personnel experienced in setting up, troubleshooting, conducting and analyzing tests on solar thermal propulsion hardware. Operates the aforementioned laboratory under various conditions to test a wide range of hardware. Equipment is kept in a high state of readiness, and personnel maintain a high degree of expertise.

DESCRIPTION OF CONCEPT

The solar thermal propulsion system consists of two primary concentrators, one or two thrusters, propellant tank, controls, sun-tracking system, and associated hardware. Sunlight is collected and focused through two apertu (180^{o} apart) from the primary concentrators. Solar ener may be further focused by secondary concentrat positioned between the primary concentrators and the thrus apertures. The thermal energy is then absorbed by a h exchanger which transfers the heat to the propellant. T propellant expands through the nozzle(s), producing thru There is no ignition or combustion of the hydrog propellant; no oxidizer is used.

Concentrators have two degrees of freedom of moveme to allow power reception and thrust simultaneously. T concentrators are required to put the center of mass on t thrust line so that spacecraft can be operated in a so thermal propulsion mode.[4] Both mirrors need to track t sun at the same time to get enough energy into the hydrog gas to expand it out the propulsive nozzle. Only one of t two mirrors need be used to track the laser to get t hydrogen gas to expand and produce thrust. There are ot variations that may be considered. Size will be determin by mission requirements for thrust and available la intensity.

ADVANTAGES

Thrust is proportional to the useful collected solar pow The higher the temperature of the system (up to t thermodynamic limit), the higher the achievable thrust. Hi Specific Impulse may be achieved; possibly 1000 sec usi hydrogen gas (cryogen) as the propellant or about 450 s using ammonia (storable) as the propellant. Almost any g can be used as the propellant: hydrogen, ammon hydrazine, helium, argon, etc. Only the propellant is carri to orbit.[5] The energy source is the sun or a ground bas laser.

The concentrator need only be as large as the laser sp size. If properly designed, the system could wo satisfactorily in either laser or solar thermal propulsion mo The entrance apertures of the secondary concentrator and t absorber can be much smaller if operated in laser therm mode. This is because laser light can be focused to a m smaller spot for the same input power. The solar mo would produce lower thrust during intervals when a la ground station was not in view. When the spacecraft eclipsed from the sun, the laser power beaming should ca it through at higher thrust, faster.

The Propulsion Directorate will test the solar mode operation on the ground using OL-AC PL/RKES existi solar thermal propulsion facilities and hardware. The la

[3] Tom Zlebek, ITT Statistical Programs Group Presentation of Taguchi Methods, 19-26 Feb 1991, based on Dr. Genuchi Taguchi's Design of Experiments.

[4] Michael R. Holmes and Kristi K. Laug, Dependence of Solar-Thermal Rocket Performance on Concentrator Performance, 1995 ASME/JSME/JSE International Solar Energy Conference Proceedings, Maui HI, 19-24 March 1995. Vol 2, pp. 837-848.

[5] Holmes and Laug

mode of operation on the ground was tested using PL/LIDB existing laser facilities and hardware.[6]

DISADVANTAGES

A cryogenic fuel is not desirable for satellite repositioning missions. A storable propellant must either be carried, made, or accessed in space to make it profitable or even possible. Most times, strictly solar powered maneuvering will be much slower than laser powered maneuvering, but more consistent, especially in the more distant orbits.

EXPERIMENTS

During the summers of 1994 and 1995 the Solar Propulsion Group at Edwards AFB worked on the design, fabrication, and test of our Reticulated Vitreous Carbon Calorimeter (RVCC) as a Volumetric Absorber Solar Engine.[7] The wafers were deemed fit to test in a harsh laser environment. They survived the testing in the Phillips Laboratory Laser Imaging Group's (PL/LIDB) Chemical Oxygen Iodine Laser (COIL) for the most part. Some wafers did receive a fair amount of damage.[8] See Figures 3 through 6 below. Figures 3 and 4 are prelased wafers. Figures 5 and 6 are the same wafers after lasing.

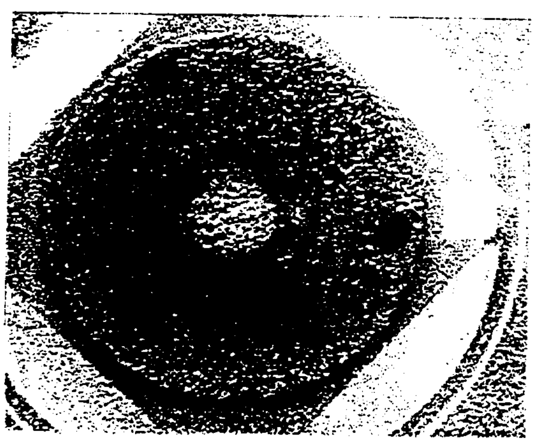

Fig. 3 Prelased Hafnium Carbide Wafer (M-13)

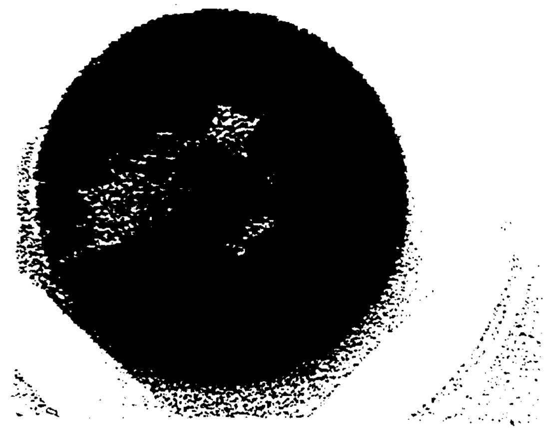

Fig. 4 Prelased Hafnium Carbide Wafer (M-13 Reverse)

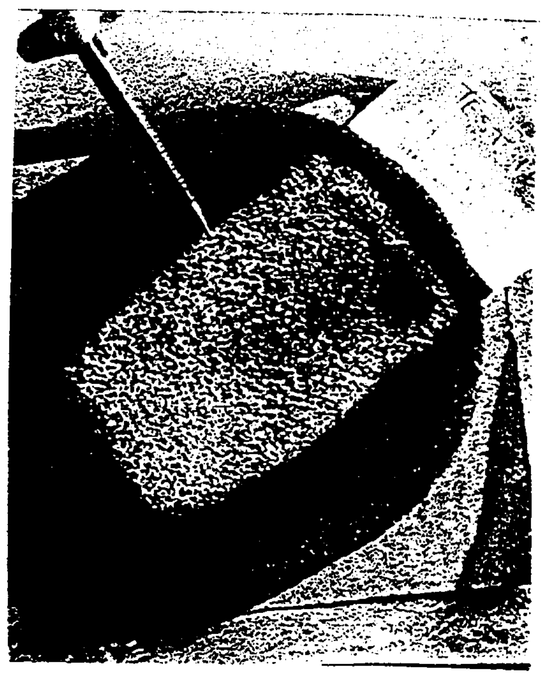

Fig. 5 Lased Hafnium Carbide Wafer (M-13)

[6] Laug & Holtzclaw, Volumetric Absorber as Solar Engine Utilizing Laser Thermal Power for Energy Input

[7] Kristi K. Laug and Alan J. Baxter, Evaluation of Hafnium-Carbide Wafers for use in a Solar Calorimeter, 13th Symposium on Space Nuclear Power and Propulsion (SNPS), Proceedings of the Space Technology and Applications International Forum (STAIF-96), 8-11 January 1996.

[8] Laug and Holtzclaw, Volumetric Absorber as Solar Engine Utilizing Laser Thermal Power for Energy Input.

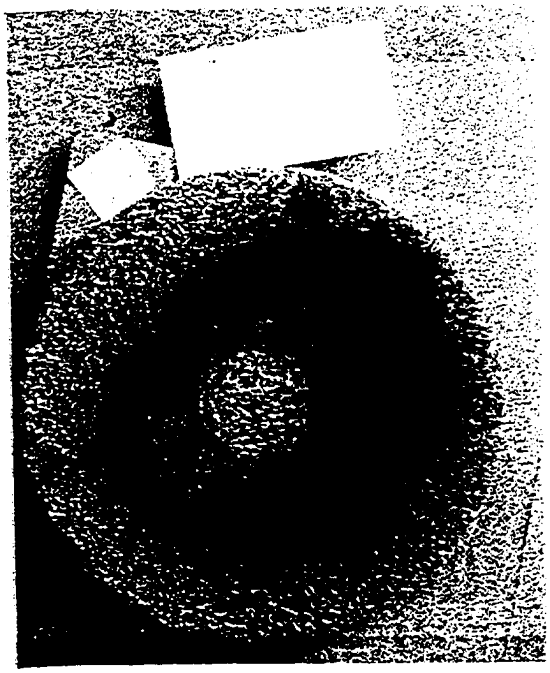

Fig. 6 Lased Hafnium Carbide Wafer
(M-13 Reverse)

Test Hardware and Setup Description

The RVCC cavity is 190.5 mm (7.5 in.) nominal internal diameter. It is approximately 457.2 mm (18 in.) in length. It converges down to 25.4 mm (1 in.) diameter at the outlet. It is not equipped with a nozzle; therefore it is not a thruster. The RVCC is made of a 203.2 mm (8 in.) stainless steel pipe and one end cap nested inside a 254 mm (10 in.) stainless steel pipe and one end cap. At the other end is a 203.2 mm (8 in.) to 254 mm (10 in.) *annular* pipe cap, joining the two pipes. The seams are all welded. Long fins were welded in a helix around the outside of the inner pipe, to direct cooling water flow. See Figure 7. Reticulated vitreous carbon and/or hafnium carbide discs are pushed in through the front behind the window (which is removable) a specified distance. See Figure 8.

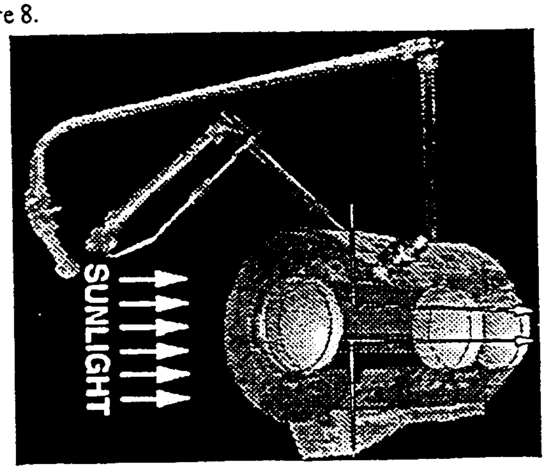

Fig. 7 RVCC Assembly Schematic

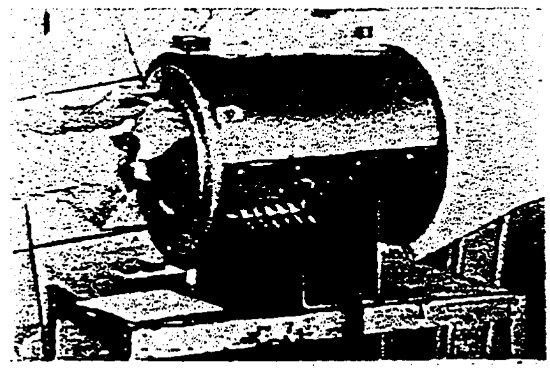

Fig. 8 RVCC Disc Installation

Helium propellant enters the front of the cavity (ar cross section) through a tube. It is held inside the c behind the quartz window. The propellant exits the opp end, through a tube to a heat exchanger.

There are 14 sealed thermocouple ports inserted th: the double walls of the RVCC, 2 each station, 180 de apart, axially. There are 12 Type C (26% tungste rhenium) thermocouples inserted into the instrumen: ports along with one pressure transducer. Seven "sta: were designated. The stations served as positioning loc: for the wafers. Two types of wafers were inserted: c (C), and hafnium carbide chemical vapor deposited ((on carbon foam blanks (HfC).

The variables are all related to physiccal characterist the wafers, or influences that affect the solar funace They include the following. The wafer porosity ranged 10 to 100 ppi. The wafer material was either carb hafnium carbide. The wafers came in three thickn 12.7 mm (.5 in., 25.4 mm (1 in.), or 50.8 mm (2 in.). from that, it is possible the position of the wafers in the the thickness of the front wafer, and the porosity c individual wafers in the stack all had bearing on the out Other considerations, such as density of the hafnium cc shape of the pores, shininess, etc., had to be lumped in signal and noise factors under thermal conduc propellant pressure through the wafers, wafer colo thermocouple reading at each station.

The solar facility itself had variables that had considered. The first and foremost obvious parameter be the sun quality. It could be a very finely tuned vari: we had set the door height at levels to exactly corre with a given power rating, but that would increase the to such a degree it was not practical. Suffice to say th heights (fully and half open for 24.7 kW and 12.3: respectively) are acceptable. The sun quality varie: seasonal variations affecting the Earth. For instance, shortest days of the year from 8 December to 8 Janua sun is not shining through as much atmosphere as it is the longest days (8 June to 8 July). However, the angle is greater because of the elliptical orbit of the earth and the 23 degree tilt of the axis. On the longest days the sun is at a more direct angle, but it is farther away. Then there are the points in between. Four basic seasons were chosen instead of months to cut down the number of factors.

Then there are several hours each day that work to vary the data. We chose 11:30am and 1:30pm because no matter the season of the year, those two times are always available as test times. 12:30pm could have been used, but again that increased the number of factors without gaining enough in return.

As for the furnace itself, propellant flowrate could have been varied infinitely. We chose three flowrates for the tests. We chose two propellants to use as the fuel (hydrogen and helium). There are many others, but we're set up for using those two.

The concentration ratio varies as the size of the primary concetrator area over the entrance aperture area of the test article (geometric). That changes over the course of the day somewhat because our heliostat is not flat, and the shape is not perfect, but assume it remains close to 8000 : 1 for the tests.

Temperature can be an important factor, controllable or not. Some data will hinge the temperatures of various coolants in the lab. Placement of thermocouples before or after or in the middle of certain stations will affect the reduced overall data.

We run a gaseous nitrogen ejector to drag the fuel molecules out of the altitude chamber. The pressure could be varied infinitely, but we chose 690 kPa to 3447 kPa (100 psi and 500 psi)

Another factor that dictates when we can test is windspeed. If the windspeed climbs to greater than 15 km per hour, the heliostat we use to track the sun bounces and causes the spot focus to move. Tracking parameters could be considered as a variable, but they were rolled into the heliostat diffusivity, intensity, and flux signal factors.

A statistical experimental design method was used to determine the test matrix. It was loosely based on Taguchi's Design of Experiments. The test matrix pitted the wafer porosity against type against power rating and propellant flow rate among other variables. The design mapped out many more parameters and variables than was practical, using Taguchi's methods. See the paragraphs below for more information.

Assumptions

The experimental data must be repeatable. In this case, it will be difficult because of dealing with changing conditions from day to day, even minute to minute. Assume that test conditions can be duplicated on a day during a given season that will be similar to the day the original data was taken.

The population follows normal distribution. Assume this to be true. Each level of a factor has identical variance. The data will be obtained at random within the seasonal constraints put on the testing.

Method

Taguchi Design of Experiments

The Taguchi Design of Experiments method is a statistical analysis method. Supposedly there are a specific number of parameters that are grouped, considered, and varied as part of the experimental design process. The idea is to shorten the number of tests, while increasing the knowledge about each test and its relationship to other tests. This is supposed to cover several items of information per test that will correlate with other sets of data from other tests. If the number of parameters grows, to cover all of the possibilites, the matrix size becomes unwieldy, making it very difficult to determine the statistical analysis of variance (ANOVA) tables.[9] If the number is lessened, the matrix becomes suspect because there may not be enough information to base a decision.

There are three basic groups of factors that must be brainstormed, shuffled, and apportioned. They are the Quality Characteristics (QCs) or parameters which directly affect the output; Signal Factors; and Noise Factors. Signal Factors are those you have some minimal control over, or can rate in numerical terms or groups that can be dealt with logically. Noise Factors are totally uncontrollable.

The following sections describe the steps were taken and how the design of experiments test matrix was accomplished. First, the subject descriptions were listed, assigned alpha numerics, and placed in a table called the Factor Group Listing. See Table 1 below.

[9]Zlebek, Taguchi Design of Experiments

Table 1 Factor Group Listing

LETTER DESIGNATION	QUALITY CHARACTERISTICS	NOISE FACTOR	SIGNAL FACTOR
A	laboratory door height (half or fully open)		
B			propellant pressure
C	propellant flow rate (.1, .3, or .6 grams per sec)		
D	wafer pore size (nominally 20, 40, 60, or 100 ppi)		
E		number wafers stacked (distance within cavity length)	
F	thickness of stacked wafers of a given ppi (1/2 in, 2 in, or 3 1/2 in thick)		
G	gaseous nitrogen ejector pressure (100 or 500 psi)		
H		concentration ratio	
I	time of day (11:30 or 13:30)		
J			
K	material (carbon-C or hafnium carbide-M)		
L			
M		thermal conductivity	
N	season (winter-30 Nov to 31 Jan, spring-1 Feb to 15 May, summer-16 May to 23 Aug, fall-24 Aug to 29 Nov)		
O			air temperature (ambient)
P			water inlet temperature
Q			propellant temperature
R			heliostat diffusivity
S			width of concentrator intensity distribution on target
T			height of concentrator intensity distribution on target
U			wafer color
V			normal incidence pyrheliometer reading (flux)
W	thermocouple placement (centered on wafer edge or between wafers		
X		propellant type (helium or hydrogen)	
Y	wafer placement (toward front or rear)		
Z		thermocouple reading at each station	
AA			wafers single or combo to get stacked height
AB	thinnest wafer position (front or rear of stack)		
AC			same wafer combo and order or different from last time particular stack used
AD			windspeed

The best way to determine the factors was to cor brainstorming session. Then levels of values and deg freedom for each one were added. If the list is too lor is, greater than the orthogonal array that can be worke eliminate some. Like variables were combined possible. The degrees of freedom are the number of minus one. Next, the appropriate orthogonal array ascertained for each group of factors in the listin signal, or noise) and the ANOVA tables determined target values. Finally, the significant variables were se The experiments will be performed as randor possible.[10] Then find out if there are any matches. point either go back to square one with a better underst of the mechanisms involved so it can be done right th time. If the experimental process is successful, t fodder for a really good paper.

While some of the reasons behind the factors group immediately apparent, some are not. For instance, combinations, or placement of a given wafer in a st wafers may not seem to have much of an impact on tl if all the wafers are the same porosity, or the same thic However, when flowing a gas over the wafers that are by convection, radiation, and conduction, there m eddies and currents introduced that could affect the Imagine how the listed interactions may occur. The c cause one wafer in the middle to cool down in one area still allowing the wafers around it to become heated. not occur if a particular wafer is moved to another pc As seen in Table 2, the QCs are very well defined in te levels, degrees of freedom, and specific values.

10 Ibid.

Table 2 QC Leveling and Degrees of Freedom Determination

ALPHA	QC's ONLY DESCRIPTION	LEVEL DESCRIPTION	LEVEL ALPHA	NUMBER OF LEVELS	DEGREES OF FREEDOM
A	door height	1/2 (half open), 1 (fully open)	A1,A2	2	1
C	propellant flow	.1, .3, .6 grams/sec	C1,C2,C3	3	2
D	wafer pore size	20, 40, 60, 100 ppi	D1,D2,D3,DD4	4	3
F	stacked height	1/2 in, 2 in, 3 1/2 in	F1,F2,F3	3	2
G	ejector pressure	500 psi, 100 psi	G1,G2	2	1
I	time of day	11:30, 13:30 test time	I1,I2	2	1
K	material	C or M	K1,K2	2	1
A x C	door vs. propellant flow interaction suspected		AC1,AC2,AC3	3	2
C x D	propellant flow vs. wafer pore size interaction suspected		CD1,CD2,CD3,CD4,CD5,CD6,CD7	7	6
C x F	propellant flow vs. stacked wafer height interaction suspected		CF1,CF2,CF3,CF4,CF5	5	4
C x I	propellant flow vs. time of day interaction suspected		CI1,CI2,CI3	3	2
N	season	W, S, S, F	N1,N2,N3,N4	4	3
W	thermocouple placements	between wafers or centered on edge	W1,W2	2	1
Y	position of wafers in cavity	toward front or rear	Y1,Y2	2	1
AB	skinny wafer position	toward front or rear	AB1,AB2	2	1
				48	31

⟹ $L_{32}(2)^{31}$

This paper is not going to describe everthing done by Taguchi's methods. That is well-defined in several volumes and treatises. However, based on the above information it can be seen how the following tables were generated. Build an ANOVA Table as seen in Table 3.

Do the same leveling and dof determination for the signal factors and noise factors using Table 2 as a guide. See the following tables (4 and 5).

Table 3 QC ANOVA Table for No Target Value Specified

SOURCE	DEGREES OF FREEDOM	LEVELS	S	V	F	S'	ρ%
A	1	2	$S_A=[(A\ level\ 1)^2/nA1+(A\ level\ 2)^2/nA2]-T^2/n$	$V_A=S_A/dof_A$	$Fn=V_A/V_e$	$S_A'=Sa-dof_A*V_e$	$\rho_A=S_A'/S_T*100$
C	2	3	$S_C=[(C\ level\ 1)^2/nC_1+(C\ level\ 2)^2/nC_2+(C\ level\ 3)^2/nC_3]-T^2/n$	$V_C=S_C/dof_C$	$Fn=V_C/V_e$	$S_C'=S_C-dof_C*V_e$	$\rho_C=S_C'/S_T*100$
D	3	4	$S_D=[(D\ level\ 1)^2/nD_1+(D\ level\ 2)^2/nD_2+(D\ level\ 3)^2/nD_3+(D\ level\ 4)^2/nD_4]-T^2/n$	$V_D=S_D/dof_D$	$Fn=V_D/V_e$	$S_D'=S_D-dof_D*V_e$	$\rho_D=S_D'/S_T*100$
F	2	3	$S_F=[(F\ level\ 1)^2/nF_1+(F\ level\ 2)^2/nF_2+(F\ level\ 3)^2/nF_3]-T^2/n$	$V_F=S_F/dof_F$	$Fn=V_F/V_e$	$S_F'=S_F-dof_F*V_e$	$\rho_F=S_F'/S_T*100$
G	1	2	$S_G=[(G\ level\ 1)^2/nG_1+(G\ level\ 2)^2/nG_2]-T^2/n$	$V_G=S_G/dof_G$	$Fn=V_G/V_e$	$S_G'=S_G-dof_G*V_e$	$\rho_G=S_G'/S_T*100$
I	1	2	$S_I=[(I\ level\ 1)^2/nI_1+(I\ level\ 2)^2/nI_2]-T^2/n$	$V_I=S_I/dof_I$	$Fn=V_I/V_e$	$S_I'=S_I-dof_I*V_e$	$\rho_I=S_I'/S_T*100$
K	1	2	$S_K=[(K\ level\ 1)^2/nK_1+(K\ level\ 2)^2/nK_2]-T^2/n$	$V_K=S_K/dof_K$	$Fn=V_K/V_e$	$S_K'=S_K-dof_K*V_e$	$\rho_K=S_K'/S_T*100$
N	3	4	$S_N=[(N\ level\ 1)^2/nN_1+(N\ level\ 2)^2/nN_2+(N\ level\ 3)^2/nN_3+(N\ level\ 4)^2/nN_4]-T^2/n$	$V_N=S_N/dof_N$	$Fn=V_N/V_e$	$S_N'=S_N-dof_N*V_e$	$\rho_N=S_N'/S_T*100$
A x C	2	3	$S_{AxC}=[(AxC\ level\ 1)^2/nAxC_1+(AxC\ level\ 2)^2/nAxC_2+(AxC\ level\ 3)^2/nAx+D51C_3]-T^2/n$	$V_{AxC}=S_{AxC}/dof_{AxC}$	$Fn=V_{AxC}/V_e$	$S_{AxC}'=S_{AxC}-dof_{AxC}*V_e$	$\rho_{AxC}=S_{AxC}'/S_T*100$
C x D	6	7	$S_{CxD}=[(CxD\ level\ 1)^2/nCxD_1+(CxD\ level\ 2)^2/nCxD_2+(CxD\ level\ 3)^2/nCxD_3+(CxD\ level\ 4)^2/nCxD_4+$	$V_{CxD}=S_{CxD}/dof_{CxD}$	$Fn=V_{CxD}/V_e$	$S_{CxD}'=S_{CxD}-dof_{CxD}*V_e$	$\rho_{CxD}=S_{CxD}'/S_T*100$
			$(CxD\ level\ 5)^2/nCxD_5+(CxD\ level\ 6)^2/nCxD_6+(CxD\ level\ 7)^2/nCxD_7]-T^2/n$				
C x F	4	5	$S_{CxF}=[(CxF\ level\ 1)^2/nCxF_1+(CxF\ level\ 2)^2/nCxF_2+(CxF\ level\ 3)^2/nCxF_3+(CxF\ level\ 4)^2/nCxF_4+$	$V_{CxF}=S_{CxF}/dof_{CxF}$	$Fn=V_{CxF}/V_e$	$S_{CxF}'=S_{CxF}-dof_{CxF}*V_e$	$\rho_{CxF}=S_{CxF}'/S_T*100$
			$(CxF\ level\ 5)^2/nCxF_5]-T^2/n$				
C x I	2	3	$S_{CxI}=[(CxI\ level\ 1)^2/nCxI_1+(CxI\ level\ 2)^2/nCxI_2+(CxI\ level\ 3)^2/nCxI_3]-T^2/n$	$V_{CxI}=S_{CxI}/dof_{CxI}$	$Fn=V_{CxI}/V_e$	$S_{CxI}'=S_{CxI}-dof_{CxI}*V_e$	$\rho_{CxI}=S_{CxI}'/S_T*100$
W	1	2	$S_W=[(W\ level\ 1)^2/nW_1+(W\ level\ 2)^2/nW_{2-on}]-T^2/n$	$V_W=S_W/dof_W$	$Fn=V_W/V_e$	$S_W'=S_W-dof_W*V_e$	$\rho_W=S_W'/S_T*100$
Y	1	2	$S_Y=[(Y\ level\ 1)^2/nY_1+(Y\ level\ 2)^2/nY_2]-T^2/n$	$V_Y=S_Y/dof_Y$	$Fn=V_Y/V_e$	$S_Y'=S_Y-dof_Y*V_e$	$\rho_Y=S_Y'/S_T*100$
AB	1	2	$S_{AB}=[(AB\ level\ 1)^2/nAB_1+(AB\ level\ 2)^2/nAB_2]-T^2/n$	$V_{AB}=S_{AB}/dof_{AB}$	$Fn=V_{AB}/V_e$	$S_{AB}'=S_{AB}-dof_{AB}*V_e$	$\rho_{AB}=S_{AB}'/S_T*100$
e	1	2	$S_e=S_T-S_A-S_C-S_D-S_F-S_G-S_I-S_K-S_N-S_{AxC}-S_{CxD}-S_{CxF}-S_{CxI}-S_W-S_Y-S_{AB}-S_m$	$V_e=S_e/dof_e$	$Fn=V_e/V_e$	$S_e'=S_e-dof_e*V_e$	$\rho_e=S_e'/S_T*100$
m	0	1		$V_m=S_m/dof_m$	$Fn=V_m/V_e$	$S_m'=S_m-dof_m*V_e$	$\rho_m=S_m'/S_T*100$
TOTAL	32	49	$S_T=S_A+Sc+S_D+D_F+S_G+S_I+S_K+S_N+S_{AxC}+S_{CxD}+S_{CxF}+S_{CxI}+S_W+S_Y+S_{AB}+S_e$	$V_T=S_T/dof_T$	$Fn=V_T/V_e$	$S_T'=S_T-dof_T*V_e$	$\rho_T=S_T'/S_T*100$

Table 4 Signal Factors Leveling and Degrees of Freedom Determination

ALPHA	SIGNAL FACTORS DESCRIPTION	LEVEL DESCRIPTION minus	0	positive	LEVEL ALPHA	NUMBER OF LEVELS	DEGREES OF FREEDOM
B	propellant pressure	low	normal	high	B1,B2,B3	3	2
O	ambient air temperature	30	70	100	O1,O2,O3	3	2
P	water inlet temperature	40	70	80	P1,P2,P3	3	2
Q	propellant temperature	<-450	-450	>-450	Q1,Q2,Q3	3	2
R	heliostat diffusivity	<100%	100%	>100%	R1,R2,R3	3	2
S	width of concentrator intensity distribution on target	narrow	normal	wide	S1,S2,S3	3	2
T	height of concentrator intensity distribution on target	high	normal	short	T1,T2,T3	3	2
U	wafer color	black	gray	taupe	U1,U2,U3	3	2
V	normal incidence pyrheliometer reading	<25 mV	25 mV	>25 mV	V1,V2,V3	3	2
AA	wafers single or combo to get stacked height		single	stacked	AA1,AA2	2	1
AC	same wafer combo and order or different from last time particular stack used		dif	same	AC1,AC2	2	1
AD	windspeed	>30 mph	30 mph	<30 mph	AD1,AD2	3	2
	TOTAL					34	22

$L_{27}(3)^{13}$

Build the Signal Factors and Noise Factors ANOVA just like for the QC ANOVA Table 3 above. Don't after the ANOVA Tables are filled in you must pc small Ss within the column together.[11] They hav impact and if done correctly, it will save time later performing the calculations on the data reductions.

Table 5 Noise Factors Leveling and Degrees of Freec Determination

ALPHA	NOISE FACTORS DESCRIPTION	LEVEL DESCRIPTION minus	0	positive	LEVEL ALPHA	NUMBER OF LEVELS	DEGREES OF FREEDOM
E	number stacked wafers	low	normal	high	E1,E2,E3	3	2
H	concentration ratio	low	normal	high	H1,H2,H3	3	2
M	thermal conductivity	low	normal	high	M1,M2,M3	3	2
X	propellant type (helium or hydrogen)	gH2		gHe	X1,X2	3	1
Z	thermocouple reading each station	<	equal	>	Z1,Z2,Z3	3	2
	TOTAL					15	9

$L_{12}(2)^{11}$

[11] Ibid.

See Figures 9 and 10 below. Thirty-two degrees of freedom (dof) requires 37 experiments to characterize, (32 combinations of QCs in an L32 Orthogonal Array plus 5 for good measure). See Table 6 for the QC Orthogonal Array.

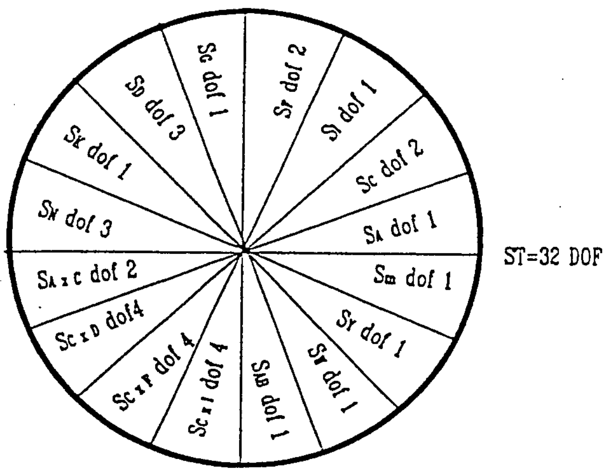

Fig. 9 QC Significant Factors Characterization Wheel

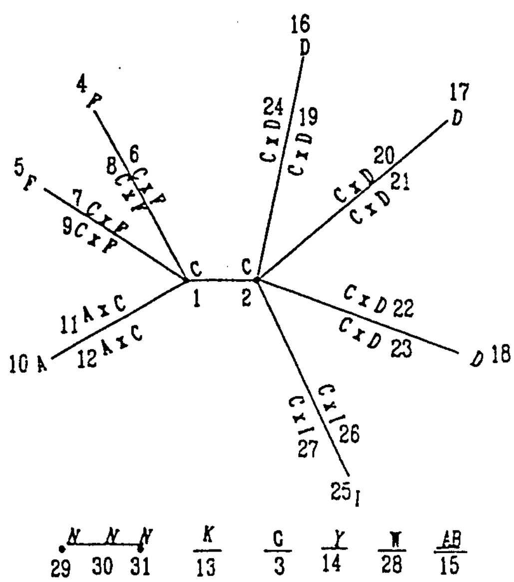

Fig 10 $L_{32}(2)^{31}$ Linear Graph for QC

Table 6 QC Factors Orthogonal Array.

dof	C (1, 2)	G (3)	F (4, 5)	C x F (6, 7, 8, 9)	A (10)	A x C (11, 12)	K (13)	Y (14)	AB (15)	D (16, 17, 18)	C x D (19–24)	I (25)	C x I (26, 27)	M (28)	N (29, 30, 31)	Y
1	1	1	1	1	1	1	1	1	1	1	1'	1	1	1	1	Y1
2	1	1	1	1	1	1	1	1	1	1'	3	2	1'	2	2	Y2
3	1	1	1	2	2	2	2	2	2	1	3	3	1'	3	2	Y3
4	1	1	1	2	2	2	2	2	2	1'	1'	1'	1	3	1	Y4
5	1	2	1'	3	3	3	3	3	3	1	1'	1'	1	2	2	Y5
6	1	2	1'	3	3	3	3	3	3	1'	3	3	1'	1	1	Y6
7	1	2	1'	1'	1'	1'	1'	1'	1'	1	3	2	1'	1	1	Y7
8	1	2	1'	1'	1'	1'	1'	1'	1'	1'	1'	1	1	2	2	Y8
9	2	3	1	1'	1	1'	1'	1'	1'	1	1'	1	1'	3	2	Y9
10	2	3	1	1'	1	1'	1'	1'	1'	1'	3	2	1	3	1	Y10
11	2	3	1	1	2	3	1	3	3	1	3	3	1	2	1	Y11
12	2	3	1	1	2	3	1	3	3	1'	1'	1'	1	1	2	Y12
13	2	1'	1'	2	3	2	2	2	2	1	1'	1'	1'	1	1	Y13
14	2	1'	1'	2	3	2	2	2	2	1'	3	3	1	2	2	Y14
15	2	1'	1'	1	1	1	3	1	1	1	3	2	1	3	2	Y15
16	2	1'	1'	1	1	1	3	1	1	2	1'	1	1'	2	1	Y16
17	3	1'	2	1'	1'	1'	1'	1	1'	3	1	1	2	3	1'	Y17
18	3	1'	2	1'	1'	1'	1'	1	1'	2	2	2	3	1	3	Y18
19	3	1'	2	3	3	1	1	2	3	3	2	3	3	2	3	Y19
20	3	1'	2	3	3	1	1	2	3	2	1	1'	2	3	1'	Y20
21	3	3	3	2	2	2	1	3	2	3	1	1'	2	3	3	Y21
22	3	3	3	2	2	2	1	3	2	2	2	3	3	2	1'	Y22
23	3	3	3	1	1	1	2	1'	1	3	2	2	3	1	1'	Y23
24	3	3	3	1	1	1	2	1'	1	2	1	1	2	1	3	Y24
25	1'	2	2	1	1'	1	2	1	1	3	1	1	3	2	1'	Y25
26	1'	2	2	1	1'	1	2	1	1	2	2	2	2	3	3	Y26
27	1'	2	2	2	3	2	1	2	2	3	2	3	2	3	3	Y27
28	1'	2	2	2	3	2	1	2	2	2	1	1'	3	2	1'	Y28
29	1'	1	3	1	2	3	1	3	3	3	1	1'	3	1	3	Y29
30	1'	1	3	1	2	3	1	3	3	2	2	3	2	1	1'	Y30
31	1'	1	3	1'	1	1'	2	1'	1'	3	2	2	2	2	1'	Y31
32	1'	1	3	1'	1	1'	2	1'	1'	1	1	1	3	3	3	Y32

The L32 and L27 Orthogonal Arrays (OA) allow substituting within the ranks. Many OAs do not. Therefore, one must be careful to choose wisely and add in error (e) columns where necessary to fill an OA correctly. Substituting may cause the OA to look unorthogonal, but they still are orthogonal.[12]

[12] Ibid.

Table 7 Estimates of Variance

$\sum_{i=1}^{n} y = T$	$\bar{y}$	y_d	$S_T = \sum_{i=1}^{n} (yi - \bar{y})^2$ [illegible]	V = [illegible] $dof_1 = (\sum (yi^2 - \bar{y})^2)/dof$	$\sigma = \sqrt{S_T/dof}$
y1	y1/1	$y_1-\bar{y}$	$yd_1^2 = y_1^2 - \Sigma(y_1)^2$	$((y_1^2 - y_1/1)^2)/dof$	$\sqrt{V}$
y2	(y1+y2)/2	$y_2-\bar{y}$	$yd_2^2 = y_1^2+y_2^2-(\Sigma(y_1+y_2))^2/2$	$((y_1^2+y_2^2-\bar{y})^2)/dof$	$\sqrt{V}$
y3	(y1+y2+y3)/3	$y_3-\bar{y}$	$yd_3^2 = y_1^2+y_2^2+y_3^2-(\Sigma(y_1+y_2+y_3))^2/3$	$((y_1^2+y_2^2+y_3^2-\bar{y})^2)/dof$	$\sqrt{V}$
y4	(y1+y2+y3+y4)/4	$y_4-\bar{y}$	$yd_4^2 = y_1+y_2+y_3+y_4-(\Sigma(y_1+y_2+y_3+y_4))^2/4$	$((y_1^2+y_2^2+y_3^2+y_4^2-\bar{y})^2)/dof$	$\sqrt{V}$
y5	(y1+y2+y3+y4+y5)/5	$y_5-\bar{y}$	$yd_5^2 = y_1+y_2+y_3+y_4+y_5-(\Sigma(y_1+y_2+y_3+y_4+y_5))^2/5$	$((y_1^2+y_2^2+y_3^2+y_4^2+y_5^2-\bar{y})^2)/dof$	$\sqrt{V}$
y6	(y1+y2+y3+y4+y5+y6)/6	$y_6-\bar{y}$	$yd_6^2 = y_1+y_2+y_3+y_4+y_5+y_6-(\Sigma(y_1+y_2+y_3+y_4+y_5+y_6))^2/6$	$((y_1^2+y_2^2+y_3^2+y_4^2+y_5^2+y_6^2-\bar{y})^2)/dof$	$\sqrt{V}$
y7	(y1+y2+y3+y4+y5+y6+y7)/7	$y_7-\bar{y}$	$yd_7^2 = y_1+y_2+y_3+y_4+y_5+y_6+y_7-(\Sigma(y_1+y_2+y_3+y_4+y_5+y_6+y_7))^2/7$	$((y_1^2+y_2^2+y_3^2+y_4^2+y_5^2+y_6^2+y_7^2-\bar{y})^2)/dof$	$\sqrt{V}$
y8	(y1+y2+y3+y4+y5+y6+y7+y8)/8	$y_8-\bar{y}$	$yd_8^2 = y_1+y_2+y_3+y_4+y_5+y_6+y_7+y_8-(\Sigma(y_1+y_2+y_3+y_4+y_5+y_6+y_7+y_8))^2/8$	$((y_1^2+y_2^2+y_3^2+y_4^2+y_5^2+y_6^2+y_7^2+y_8^2-\bar{y})^2)/dof$	$\sqrt{V}$
y9	(y1+y2+y3+y4+y5+y6+y7+y8+y9)/9	$y_9-\bar{y}$	$yd_9^2 = y_1+y_2+y_3+y_4+y_5+y_6+y_7+y_8+y_9-(\Sigma(y_1+y_2+y_3+y_4+y_5+y_6+y_7+y_8+y_9))^2/9$	$((y_1^2+y_2^2+y_3^2+y_4^2+y_5^2+y_6^2+y_7^2+y_8^2+y_9^2-\bar{y})^2)/dof$	$\sqrt{V}$
yn	(y1+y2+y3+y4+y5+y6+y7+y8+y9+yn)/n	$y_n-\bar{y}$	$yd_n^2 = y_1+y_2+y_3+y_4+y_5+y_6+y_7+y_8+y_9+\ldots+y_n-(\Sigma(y_1+y_2+y_3+y_4+y_5+y_6+y_7+y_8+y_9+\ldots+y_n))^2/n$	$((y_1^2+y_2^2+y_3^2+y_4^2+y_5^2+y_6^2+y_7^2+y_8^2+y_9^2+\ldots+y_n^2-\bar{y})^2)/dof$	$\sqrt{V}$
$\sum y$	$(\sum y_i)/n$		$=\sum (y_i)^2$	V	σ

The previous Table 7 shows the estimates of varian is the total variation, which is the sum of the square the deviations of a sample, including the error and th (if there is one). Y_d is the deviation which is the inc sample minus the mean value of y or $\bar{y}$. T is the sun the samples. $\bar{y}$ is the mean value of y which is a where n is the total number of samples.[13]

Estimates of Variance or E(V).

$$E(V_A)=\sigma_e^2+r\sigma_A^2 \quad (1$$

where r is the number of units in each level of A.

$$E(V_e)=\sigma_e^2 \quad (2)$$

$$\sigma_A^2 = V_A-\sigma_e^2. \quad (3)$$

$$\sigma_e^2 = \sum_{i=1}^{n}(y_i-\bar{y})^2 / dof. \quad (4)$$

Shortcomings

The biggest problem encountered was that there we many variables that seemed important to include one w another, it was very hard to weed them out. See Hardware and Setup Description above. The parameter which directly affects the output became very large (signal factors and noise factors), and seemingly impossit correlate to get a realistic orthogonal array.[14] There some were combined, making the results less than optir Then after the matrix was set, the laser testing damage a more variables, which were unable to be characterized. is going to be a fault in the analysis unless there is some to take care of it.

The Taguchi method is so labor intensive and subjecti nature that it is impossible to think of all the parameter even put them in the matrix because of the me limitations (have to keep the ANOVA Table sm Therefore, more tests may have to be performed later.

Test Matrix

The following Table 8 shows the final test m generated from the Taguchi Design of Experiments routine

[13] Ibid.
[14] Ibid.

Table 8 Complete Test Matrix

Test #	season	propellant	flow rate	wafer material	pore size	# wafers	station	wafer place.	wafer spacing	wafer number	station	wafer place.	wafer spacing	wafer number	station	wafer place.	wafer spacing	wafer number	station	wafer place.	wafer spacing	wafer number	station	wafer place.	wafer spacing	wafer number	station	wafer place.	wafer spacing	wafer number	station	wafer place.	wafer spacing	wafer number
1	winter	helium	.6 gps	carbon	40 ppi	2	1		1 in	C7	2	centered	1 in	C8	3	centered			4				5				6				7			
2	winter	helium	.1 gps	carbon	23.5 ppi	1	1				2	centered	1/2 in	C14	3				4				5				6				7			
3	winter	helium	.6 gps	carbon	21 ppi	2	1				2				3				4				5	between	1 in	M8	6	between	1 in	M15	7			
4	winter	helium	.3 gps	hafnium carbide	37 ppi	4	1				2				3	between	1/2 in	M3	4	between	1 in	M17	5	between	1 in	M10	6	between	1 in	M9	7			
5	winter	helium	.6 gps	carbon	23.5 ppi	1	1				2				3				4				5				6				7	centered	1/2 in	C14
6	winter	helium	.3 gps	hafnium carbide	37 ppi	4	1	between	1 in	M8	2	between	1 in	M18	3	between	1 in	M17	4	between	1/2 in	M3	5				6				7			
7	winter	helium	.6 gps	carbon	23.5 ppi	1	1				2				3				4				5				6				7	centered	1/2 in	C14
8	winter	helium	.1 gps	carbon	23.5 ppi	1	1				2	centered	1/2 in	C14	3				4				5				6				7			
9	winter	helium	.6 gps	carbon	40 ppi	2	1				2	centered	1 in	C7	3	centered	1 in	C8	4				5				6				7			
10	spring	helium	.1 gps	carbon	10 ppi	1	1	between	1/2 in	C18	2				3				4				5				6	between	1/2 in	C18	7			
11	spring	helium	.6 gps	carbon	10 ppi	1	1				2				3				4	between	1 in	C2	5	between	1/2 in	C3	6	between	1/2 in	C3	7			
12	spring	helium	.1 gps	carbon	45 ppi	3	1				2				3				4	between	1 in	C2	5	between	1/2 in	C3	6	between	1/2 in	C3	7			
13	spring	helium	.1 gps	carbon	45 ppi	3	1				2				3	centered	1 in	M14	4	centered	1 in	M13	5	centered	1 in	M7	6	centered	1/2 in	M1	7			
14	spring	hydrogen	.1 gps	hafnium carbide	44 ppi	4	1				2	centered	2 in	M12&M10	3	centered	1 in	M11	4	centered	1/2 in	M16	5				6				7			
15	spring	hydrogen	.3 gps	hafnium carbide	45 ppi	4	1				2				3				4				5	centered	1/2 in	M18	6	centered	1 in	M10	7	centered	2 in	M12&M11
16	spring	helium	.1 gps	hafnium carbide	9 ppi	4	1				2				3				4				5				6				7			
17	spring	helium	.1 gps	carbon	10 ppi	1	1	between	1/2 in	C18	2				3				4				5				6				7			
18	spring	helium	.6 gps	carbon	45 ppi	1	1				2				3				4				5				6	between	2 in	C1	7			
19	spring	helium	.1 gps	carbon	45 ppi	3	1				2	centered	1/2 in	C8	3	centered	1 in	C4	4				5				6				7			
20	summer	hydrogen	.1 gps	hafnium carbide	9 ppi	1	1				2	between	1/2 in	M1	3				4				5				6				7			
21	summer	helium	.1 gps	hafnium carbide	44 ppi	3	1				2				3				4	between	1/2 in	M8	5	between	1/2 in	M18	6	between	1 in	M11	7			
22	summer	hydrogen	.1 gps	hafnium carbide	44 ppi	2	1				2				3				4				5				6	between	1 in	M11&M12				
23	summer	helium	.3 gps	carbon	10 ppi	2	1				2	centered	1 in	C15	3	centered	1 in	C18	4				5				6				7			
24	summer	helium	.6 gps	hafnium carbide	44 ppi	2	1	between	1 in	M11	2	between	1 in	M12	3				4				5				6				7			
25	summer	helium	.3 gps	carbon	10 ppi	1	1				2				3				4				5				6				7			
26	summer	helium	.6 gps	hafnium carbide	45 ppi	2	1				2				3				4				5				6	centered	1/2 in	C18	7			
27	summer	helium	.3 gps	carbon	10 ppi	1	1				2				3				4				5				6				7			
28	summer	helium	.1 gps	carbon	10 ppi	3	1				2	centered	1/2 in	C8	3	centered	1 in	C4	4	centered	2 in	C1	5				6				7			
29	summer	helium	.3 gps	carbon	37 ppi	2	1				2	centered	1 in	C15	3	centered	1 in	C18	4				5				6				7			
30	fall	helium	.6 gps	hafnium carbide	23.5 ppi	2	1				2	centered	1 in	M9	3	centered	1 in	M17	4				5				6				7			
31	fall	helium	.6 gps	carbon	23.5 ppi	1	1				2				3				4				5				6	between	1/2 in	C14	7			
32	fall	helium	.3 gps	carbon	23.5 ppi	4	1	between	1 in	C11	2	between	1 in	C12	3	between	1 in	C13	4	between	1/2 in	C14	5				6				7			
33	fall	helium	.1 gps	hafnium carbide	21 ppi	1	1				2	centered	1/2 in	M4	3				4				5				6				7			
34	fall	hydrogen	.1 gps	hafnium carbide	37 ppi	2	1				2	centered	1 in	M9	3	centered	1 in	M7	4				5				6				7			
35	fall	helium	.3 gps	carbon	40 ppi	4	1	between	1/2 in	C10	2	between	1 in	C9	3	between	1 in	C8	4	between	1 in	C7	5				6				7			
37	fall	helium	.3 gps	carbon	23.5 ppi	4	1	between	1 in	C11	2	between	1 in	C12	3	between	1 in	C13	4	between	1/2 in	C14	5				6				7			
38	fall	helium	.3 gps	carbon	40 ppi	4	1	between	1/2 in	C10	2	between	1 in	C9	3	between	1 in	C8	4	between	1 in	C7	5				6				7			
39	fall	helium	.6 ppi	carbon	23.5 ppi	1	1				2				3				4				5				6	between	1/2 in	C14	7			
40	winter	helium	.1 gps	carbon	60 ppi	2	1				2				3				4				5	centered	1 in	C7	6	centered	1 in	C8	7			
41	winter	helium	.1 gps	carbon	60 ppi	2	1				2				3				4	centered	1 in	C8	5	centered	1 in	C8	6				7			

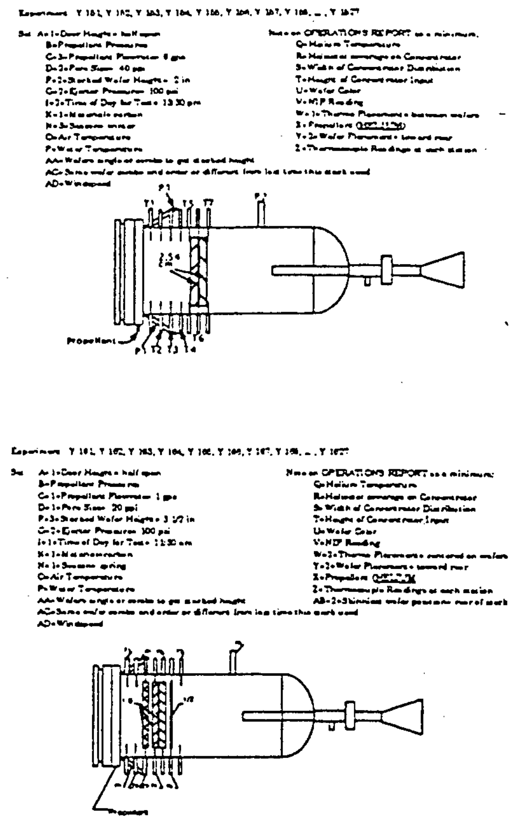

Fig. 11 Two Examples of Wafer Placement During Experiments

RESULTS/CONCLUSIONS

There aren't any results yet because no tests have been performed to date. Testing will take over a year to complete; tests are planned over the course of four seasons.

By using the Taguchi DOE, we expect to cut down the number of experiments from greater than 140 down to less than 40. This will save time, energy, and money in terms of tests, propellant, manhours, and computer time. At the same time, it should give us more useful and correlatable data.